



# Longitudinal Seismic Analysis of Large-Diameter Shield Tunnels in the Regions that have High Seismic Intensity

Bo Li<sup>1\*</sup>, Xiaoqin Shen<sup>2a</sup>

<sup>1</sup>CCCC Second Highway Consultant Co. Ltd, Wuhan, China

<sup>2</sup>HUBEI WATER RESOURCES TECHNICAL COLLEGE, Wuhan, China

\*410377174@qq.com, <sup>a</sup>150365777@qq.com

**ABSTRACT.** Since earthquake hazards are seriously threatening economy and sustainable development, it is particularly significant to study the seismic analysis of large-diameter shield tunnels in regions with high seismic intensity to ensure the seismic safety of the tunnels. This study is based on an overseas large-diameter shield tunnel project as a background in which the normative response spectrum was obtained according to Chinese codes and local codes. According to the selected 6 effective seismic waves, the dynamic time history analysis method was applied to select the typical cross section of the longitudinal tunnel section. A two-dimensional finite element model was established for the surrounding soil to analyze the overall force and deformation of the shield tunnel under the action of the earthquake, internal force of the tunnel rings and uneven settlement etc., in order to analyze the rationality and feasibility of the design.

**Keywords:** High seismic intensity; shield tunnel; seismic waves; dynamic time history analysis

## 1 Introduction

With the rapid development of urbanization, there are more and more large-diameter shield tunnel projects, and the regional distribution is becoming wider and wider<sup>[1][2][3]</sup> (CAI 2020,GENG 2007,KONG 2010). It is of great significance to carry out seismic research on underground structures in areas with high seismic intensity to ensure their seismic safety. Therefore, it is necessary to analyze the dynamic time history of large-diameter shield tunnels under the action of earthquakes, calculate the relevant content of earthquake resistance, and analyze the rationality and feasibility of the design. Earthquakes have strong randomness<sup>[4][5][6][7]</sup>(LIU 2019,LIANG 2017,LIANG 2014,Liu 2023).Analysis shows<sup>[8][9][10]</sup>(SHAO 2013,XUE 2020,YAN 2010) that the seismic response of structures varies greatly with the input seismic waves, and the difference is as high as several times or even ten times. Therefore, in order to ensure the rationality of the time-history analysis results, the input seismic waves must be selected reasonably.

This paper is based on an overseas large-diameter shield tunnel project, according to Chinese codes and local codes, and combined with the site conditions of the project

© The Author(s) 2023

Z. Ahmad et al. (eds.), *Proceedings of the 2023 5th International Conference on Structural Seismic and Civil Engineering Research (ICSSCER 2023)*, Atlantis Highlights in Engineering 24,

[https://doi.org/10.2991/978-94-6463-312-2\\_32](https://doi.org/10.2991/978-94-6463-312-2_32)

to obtain the normative response spectrum; MATLAB programming is used to calculate the artificial waves corresponding to the normative response spectrum; SeismoSignal software is used to calculate the response spectrum of the natural waves compared with the standard spectrum, and the appropriate natural waves are selected. The three-dimensional dynamic model is used to analyze the overall stress and deformation of the shield tunnel in saturated sand under the action of earthquake, the internal force of the tunnel ring segments, the internal force of the segment joints, and the uneven settlement.

## 2 Project Overview

The overseas project tunnel is located in the river which is about 1075m wide, and the total length of the tunnel is about 3400m, of which the shield section is 2450m long, the shield outer diameter is 11.8m, the thickness of the C60 reinforced concrete segment is 0.5m, and the ring width is 2m. It is assembled by staggered joints. It is connected by 46 pieces of M30 oblique bolts in the circumferential direction.

The exploration stratum in the tunnel site area is divided into 8 major layers. The shield section mainly passes through strong permeable layers such as silty fine sand and silt. The geological section is shown in Figure 1. The project site is the third group of III class sites, with an earthquake design intensity of 8 degrees (design basic seismic acceleration is 0.20g), the tunnel is designed according to ground motion parameters with a probability of exceeding 10% in the 100-year base period, and the peak acceleration is 0.22g.



Fig. 1. Geological Profile

## 3 Seismic waves selection and model establishment

### 3.1 Selection of seismic waves

The analysis of this project adopts 7 groups of natural waves that conform to the characteristics of the site, namely EL Centro, Type1, Type2, Type3, Type4, Type5, and Type6 seismic waves. Among them, Type1, Type2 and Type3 are provided by AECOM; the corresponding numbers of Type4, Type5 and Type6 are 832, 928 and 1147 respectively, which are recommended by the international consultant company.

A total of 6 seismic conditions were calculated, see Table 1. Seismic waves are applied in both x and y directions, the peak acceleration of seismic waves in the x direction is 0.22g, and the peak acceleration of seismic waves in the y direction is calculated as x direction: y direction=1:0.65. The seismic wave waveforms in the x and y

directions from working conditions 1 to 4 are the same, but the peak accelerations are different. Different seismic waves are used in the x and y directions of working conditions 5 to 6. Except for case 4, the seismic waves are artificial waves, and other cases used natural waves.

The seismic acceleration time-history curves are shown in Figures 2 to 3, where the horizontal axis indicates time (s) and the vertical axis indicates acceleration ( $m/s^2$ ).

**Table 1.** Seismic conditions

Seismic condition	Seismic waves	Remarks
1	El Centro wave	Waveforms of seismic waves in the direction of x and y are the same.
2	Type1	
3	Type3	
4	Artificial wave	
5	Type4	Different seismic waves are used in the direction of x and y.
6	Type5	

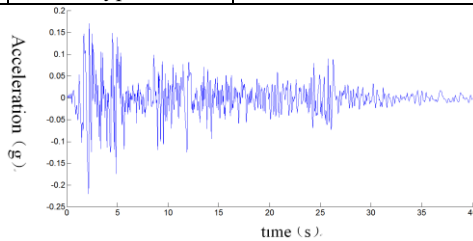


**Fig. 2.** El Centro seismic wave

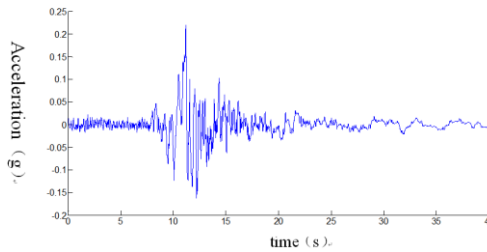


**Fig. 3.** Type1

### 3.2 Model simplification principles and dimensions

Taking the section KZ3+620 for calculation, the width is 400m, the depth taken in the direction of the stratum towards the bedrock is 80m.

The models for soil and segment materials are selected according to linear elasticity, the soil is simulated by plane strain element, the segment is simulated by beam element, and the tunnel finite element calculation is performed according to the elastic mechanics plane strain problem.

Under the action of ground motion, the internal force of the shield segment will change. In the structural calculation, the internal force of the four feature points A, B, C, and D of the tunnel section is extracted to show the time-history curve of the change of the internal force of the segment under the action of the earthquake. The location of the feature points is shown in Figure 4 below.

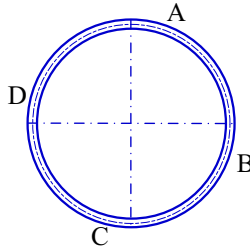


**Fig. 4.** Schematic diagram of the calculation of the location of the feature points of the shield tunnel

### 3.3 Model Boundary Condition Settings

When carrying out the self-weight stress balance calculation, the bottom surface of the model is fixed, the normal displacement is constrained on both sides, and the upper surface is unrestrained. During seismic calculation, the bottom surface, both sides and upper surface of the model are unrestrained, and seismic waves are applied to the bottom surface of the model.

### 3.4 Material Models and Parameters

The segment structure adopts C60, elastic modulus=36000MPa, Poisson's ratio=0.167.

The soil material parameters are shown in Table 2:

**Table 2.** The value of soil elastic modulus, Poisson's ratio and density

Soil layer	Compressive modulus (MPa)	Poisson's ratio	Static elastic modulus (MPa)	Dynamic elastic modulus (MPa)	Dynamic Poisson's ratio	Density (kg/m <sup>3</sup> )
②	1	0.4	0.5	2	0.48	1810
③6	20	0.29	15.3	61.2	0.4	1830
③8	25	0.28	19.6	78.4	0.4	1890
④	30	0.28	23.5	94	0.4	1860
⑤2	35	0.28	27.4	109.6	0.4	1850

### 3.5 Calculation of the load

The calculated load is the self-weight of the structure + the seismic load. The importance coefficient of structure takes  $0=1.1$ , the sub-item coefficient of self-weight load takes 1.0, the sub-item coefficient of earthquake load takes 1.0, and the acceleration of gravity takes  $9.8m/s^2$ .

Seismic waves are applied in two directions of x:y, the peak acceleration of seismic waves in x direction is 0.22g, and the peak acceleration of seismic waves in y direction is calculated to be x direction: y direction=1:0.65. The seismic wave waveforms in the x and y directions from working conditions 1 to 4 are the same, but the peak accelerations are different. Different seismic waves are used in the x and y directions from working conditions 5 to 6.

## 4 Computational Structural Analysis

### 4.1 Internal force time history curve

Taking the bidirectional seismic case 1 as an example, the internal force time-history curves of each calculation point are shown in Figures 5.

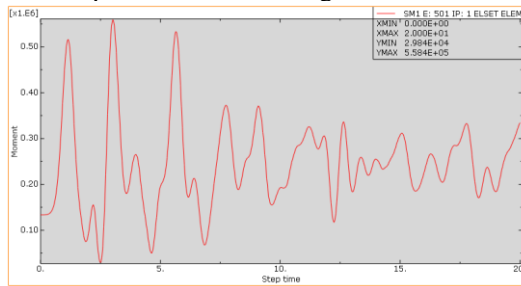


Fig. 5. Bending moment time history curve at point A (N · m/m)

### 4.2 Internal force diagram of tunnel segment

The maximum bending moment at point A occurs at time 3s. At this time, the internal force of the tunnel segment is shown in Figure 6

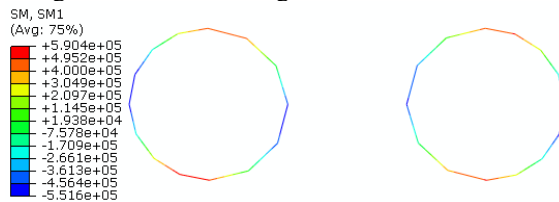


Fig. 6. Segment bending moment(N · m/m) at Time 3s

### 4.3 Deformation time-history curve

The vertical relative displacement of point A and point C is shown in Figure 7.

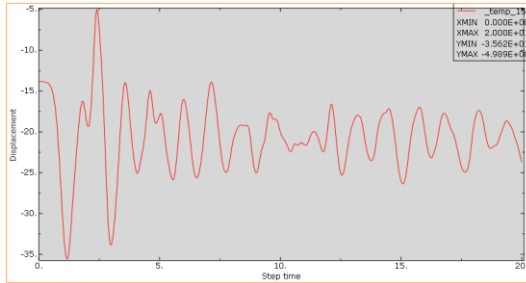


Fig. 7. Vertical relative displacement of point A and point C(mm)

### 4.4 Result analysis

Table 3 compares and lists the maximum internal force of each feature point during the simultaneous action of multidirectional ground motions.

Table 4 lists the internal force peaks of each feature point in the one-way action and multi-direction simultaneous action of the El Centro seismic wave. It can be seen that when multiple directions act at the same time, the internal force of the structural ground motion is larger than that when acting in one direction.

Table 5 compares and lists the maximum relative displacements of feature points A and C during the simultaneous action of multidirectional ground motions.

Table 3. List of internal force peaks of each feature point

Location	Bending moment (KN·m/m)	Axial force (KN/m)	Shear force (KN/m)	Seismic wave type
A	558.4	2579	151.4	El Centro
	671.5	2604	322	Type1
	592.2	2631	303.9	Type3
	872.8	2903	336.8	artificial waves
	531.3	2386	190.7	Type4
	524.9	2343	86.83	Type5
B	481.9	4297	258.5	El Centro
	697.2	4525	384.1	Type1
	609.7	4531	316.1	Type3
	793.3	5051	409	artificial waves
	510.2	4192	231.6	Type4
	498.6	3810	157.2	Type5
C	507.3	2956	285.9	El Centro
	717.8	3008	422	Type1
	625.4	2938	243.3	Type3
	836.2	3123	452	artificial waves

	501.4	2828	245.6	Type4
	486	2758	136.8	Type5

**Table 4.** Comparison of unidirectional earthquake action and multi-directional earthquake action

Location	Bending moment (KN·m/m)	Axial force (KN/m)	Shear force (KN/m)
A	463.3	2471	122.7
	344.6	2216	102.5
B	569.2	3185	136.3
	238.5	2947	907.9
C	589.4	3029	92.14
	259.6	2794	423.8

**Table 5.** List of relative displacement peaks of feature points A and C

Seismic wave type	Peak relative displacement of feature points A and C(mm)
El Centro	35.62
Type1	36.8
Type3	36.89
artificial waves	39.2
Type4	37.5
Type5	36.9

Under the simultaneous action of multi-directional ground motion with a probability of exceeding 10% in one hundred years, the maximum hoop bending moment of the shield tunnel segment feature point is 872.8kN m/m, the maximum hoop axial force is 5051kN/m, and the maximum shear force is 452kN /m. The maximum relative displacement of feature points A and C is 39.2 mm, and the relative deformation is 0.363%.

By comparing the internal force values of the seismic conditions with the basic combination and the standard combination, it can be seen that the internal force values of the seismic conditions do not exceed the maximum ultimate bearing capacity, but the relative displacement of the feature points is relatively large. It is recommended to adopt corresponding seismic structural measures in structural design to improve the overall seismic capacity of the structure. In order to make the structure integral and continuous, necessary measures should be taken in the design of the fabricated reinforced concrete structure to strengthen the connection between segments.

## 5 Conclusion

According to the actual project, this paper adopts the dynamic time history analysis method for the 6 effective seismic waves selected. The typical section of the longitudinal tunnel section and the surrounding soil is selected to establish a

two-dimensional finite element model in order to analyze the overall stress of the shield tunnel under the action of earthquake. The rationality and feasibility of the design are analyzed based on the deformation, the internal force of the tunnel ring segment and the uneven settlement. Through the above analysis, the following conclusions are drawn:

(1) The ground motion is strongly random, and the seismic response of the structure varies greatly depending on the different input seismic waves. Although the artificial waves meet the requirements of the site characteristics and the design specification response spectrum, comparing with other seismic waves, their internal force value varies greatly.

(2) When the multi-directional ground motion acts simultaneously, the internal force of the structural ground motion is larger than that of the one-directional ground motion.

(3) Since the relative displacement of the structure is relatively large under earthquake conditions, corresponding seismic structural measures should be taken in the structural design to improve the overall seismic capacity of the structure.

## REFERENCES

1. CAI Xin, LIANG Jianwen, XU Anquan, LI Dongqiao, WU Zequn, YAN Qichao (2020) Longitudinal seismic analysis of Mawan sea-crossing large diameter shield tunnels. *Journal of Natural Disasters*, 29(06):13-20.
2. GENG Ping, HE Chuan, YAN Qixiang (2007). Analysis of longitudinal seismic response of shield tunnel. *Journal of Southwest Jiaotong University*,42(3) :283 – 287.
3. KONG Ge (2010). Longitudinal seismic response analysis of shield section of Wuhan Changjiang tunnel. *Building Structures*,44(S): 694 – 698.
4. LIU Jingbo, WANG Dongyang, TAN Hu, et al. (2019) Response displacement methods for longitudinal seismic response analysis of tunnel structures. *Journal of Vibration and Shock*, 38(21): 104-111,132.
5. LIANG Jianwen, LIANG Jiali, ZHANG Ji, et al. (2017) Nonlinear seismic response of 3D canyon in deep soft soils. *Chinese Journal of Geotechnical Engineering*, 39(7): 1196-1205.
6. LIANG Jianwen, YU Jungang, ZHANG Ji, et al (2014). A nonlinear seismic response analysis model for underground tunnels based on the viscous-spring boundary. *China Earthquake Engineering Journal*,36(3) :434-440.
7. Liu Lei; Xu Chengshun; Du Xiuli;Iqbal Kamran (2023). Longitudinal seismic response of shield tunnel: A multi-scale numerical analysis. *Tunnelling and Underground Space Technology incorporating Trenchless Technology Research*.Volume 138, Issue.
8. SHAO Yumeng, LEIYang (2013). Longitudinal seismic analysis of shield tunnel based on reaction displacement method. *China Civil Engineering Journal*,46(Supp2):260-265.
9. XUE Guangqiao, GUO Zhiming, YU Haitao, LUO Chiheng (2020) Quick and Practical Method for Longitudinal Seismic Analysis of Shield Tunnel. *Modern Tunneling Technology*, 57(S1):588-595.
10. YAN Qixiang, LIU Ji, ZHAO Shike, et al (2010). Application of response displacement method in longitudinal seismic analysis of shield tunnel. *Railway Engineering*, (7):77-80.



**Open Access** This chapter is licensed under the terms of the Creative Commons Attribution-NonCommercial 4.0 International License (<http://creativecommons.org/licenses/by-nc/4.0/>), which permits any noncommercial use, sharing, adaptation, distribution and reproduction in any medium or format, as long as you give appropriate credit to the original author(s) and the source, provide a link to the Creative Commons license and indicate if changes were made.

The images or other third party material in this chapter are included in the chapter's Creative Commons license, unless indicated otherwise in a credit line to the material. If material is not included in the chapter's Creative Commons license and your intended use is not permitted by statutory regulation or exceeds the permitted use, you will need to obtain permission directly from the copyright holder.

